A&A 394, 1–5 (2002)
DOI: 10.1051/0004-6361:20021066

Astronomy & Astrophysics

Optically-selected clusters at $0.8 \lesssim z \lesssim 1.3$ in the EIS cluster survey

C. Benoist[1], L. da Costa[2], H. E. Jørgensen[3], L. F. Olsen[3], S. Bardelli[4], E. Zucca[4], M. Scodeggio[5], D. Neumann[6], M. Arnaud[6], S. Arnouts[2], A. Biviano[7], and M. Ramella[7]

[1] Observatoire de la Côte d'Azur, CERGA, BP 229, 06304 Nice Cedex 4, France
[2] European Southern Observatory, Karl-Schwarzschild-Str. 2, 85748 Garching b. München, Germany
[3] Astronomical Observatory, University of Copenhagen, Juliane Maries Vej 30, 2100 Copenhagen, Denmark
[4] INAF - Osservatorio Astronomico di Bologna, via Ranzani 1, 40127 Bologna, Italy
[5] Istituto di Fisica Cosmica – CNR, Milano, Italy
[6] SAp, CEA/Saclay, L'Orme des Merisiers, Bât. 709, 91191 Gif-sur-Yvette Cedex, France
[7] INAF – Osservatorio Astronomico di Trieste, Via G. B. Tiepolo 11, 34131 Trieste, Italy

Received 7 December 2001 / Accepted 19 July 2002

Abstract. This paper presents preliminary results of a spectroscopic survey being conducted at the VLT of fields with optically-selected cluster candidates identified in the EIS I-band survey. Here we report our findings for three candidates selected for having estimated redshifts in the range $z = 0.8$–1.1. New multi-band optical/infrared data were used to assign photometric redshifts to galaxies in the cluster fields and to select possible cluster members in preparation of the spectroscopic observations. Based on the available spectroscopic data, which includes 147 new redshifts for galaxies with $I_{AB} \lesssim 22$–23, we confirm the detection of four density enhancements at a confidence level >99%. The detected concentrations include systems with redshifts $z = 0.81$, $z = 0.95$, $z = 1.14$ and the discovery of the first optically-selected cluster at $z = 1.3$. The latter system, with three concordant redshifts, coincides remarkably well with the location of a firm X-ray detection ($>5\sigma$) in a ∼80 ksec XMM-Newton image taken as part of this program which will be presented in a future paper (Neumann et al. in prep.). The $z > 1$ systems presented here are possibly the most distant identified so far by their optical properties alone.

Key words. galaxies: clusters: individual: EIS0046-2930, EIS0533-2412, EIS0954-2023 – large-scale structure of Universe – cosmology: observations

1. Introduction

Clusters of galaxies are both ideal sites for studying galaxy evolution and important cosmological probes, especially at redshifts $z \gtrsim 0.5$, where differences between competing evolutionary and cosmological models become important. This has motivated several searches for distant clusters using a variety of techniques in different wavelengths. As a result, over the past few years a remarkable progress has been made in detecting an ever increasing number of systems with $z \gtrsim 0.5$ (see Gioia 2000 for a recent review). More recently, a handful of clusters at $z \gtrsim 1$ have also been identified. While the sheer existence of these high redshift clusters is of great importance, the current number of confirmed systems is still very small, mostly identified from serendipitous X-ray searches (e.g., Rosati et al. 1999) or from infra-red imaging (Stanford et al. 1997). Therefore, the construction of a large sample of confirmed clusters at $z \gtrsim 0.8$ representative of the entire population of these high-z systems remains an important goal of observational cosmology. However, as these systems are expected to be rare, finding them requires large areas of the sky to be covered, limiting the techniques that can be used in identifying candidates. In particular, surveys at X-ray and mm wavelengths (Carlstrom et al. 2000) are unlikely to provide in the near future the necessary sky coverage for constructing the large samples of very distant clusters of galaxies required for statistical analysis.

An alternative way is to consider multi-band optical/infrared imaging data. Thanks to the advent of panoramic CCD imagers, wide-angle imaging surveys in the optical and near infrared wavelengths have become viable and can be used for identifying cluster candidates up to $z \sim 1$. Examples of wide-angle surveys that have been used to identify intermediate to high redshift clusters include those of Gunn et al. (1986), Postman et al. (1996), the ESO Imaging Survey (EIS) Cluster Survey (Olsen et al. 1999a,b; Scodeggio et al. 1999), the Red-Sequence Survey (Gladders & Yee 2000) and the Las Campanas distant cluster survey (Gonzalez et al. 2001). These surveys, especially those carried out in a single passband, can only provide plausible candidates and further progress benefits from additional multi-wavelength observations to mitigate many of the problems of foreground-background contamination, to assign photometric redshifts for

galaxies of different morphological types and to select possible cluster members to improve the yield of spectroscopic follow-ups.

In this paper we describe our first attempts to explore the nature of the high redshift cluster candidates identified in the EIS *I*-band survey, combining new imaging and spectroscopic observations. Altogether there are about 82 candidates with matched-filter redshifts $\gtrsim$0.8 for which about half have already been complemented by imaging observations in *BVRJK*. Among the various clusters for which we have spectroscopic data, we present here three clusters at higher redshift. In Sect. 2 we describe the selection of the candidate clusters and of the galaxy sample used in the observations. In Sect. 3, we briefly describe the reduction procedure which will be expanded in a separate paper where the accumulated data are presented (Jørgensen et al. in prep.). In Sect. 4, the observed redshift distribution and the technique used to identify groups in redshift space are presented. Finally, in Sect. 5 our main results are summarised.

2. Cluster and Galaxy sample

The results presented here are part of an ongoing comprehensive effort to identify and study clusters at different epochs using as a starting point the EIS cluster candidate compilation. This sample, consisting of over 300 candidates, has been split roughly into three redshift domains – low ($z \lesssim 0.4$), intermediate ($0.4 \lesssim z \lesssim 0.7$) and high ($z \gtrsim 0.7$). Several photometric and spectroscopic follow-up programs are underway at different facilities to secure the necessary data for confirmation (e.g., Olsen et al. 2001) and more detailed studies. The observations include moderately deep optical/infrared imaging in *R* and *JK* (Scodeggio et al. in prep.), spectroscopic observations of intermediate redshift clusters at the ESO 3.6 m telescope (Ramella et al. 2000; Biviano et al. in prep.), deep multi-band imaging (Schirmer et al. in prep.) for cosmic shear analysis and spectroscopic observations of high redshift candidates at the VLT, and for one case XMM-Newton data (Neumann et al. in prep.). In the present paper we focus our attention on three high-redshift ($z \gtrsim 0.8$) candidates – EIS0046-2930, EIS0954-2023 and EIS0533-2412 (Olsen et al. 1999b; Scodeggio et al. 1999) – for which photometric, spectroscopic and, in one case, X-ray data are available.

The sample of objects selected for the spectroscopic observations in the fields considered were drawn from an area of 10×10 arcmin centred at the position of the candidate clusters as determined by the matched-filter analysis of the *I*-band data. For EIS0046-2930 and EIS0954-2023 the full area is covered in *BVI*, from publicly available EIS-WIDE and/or EIS-Pilot data (Nonino et al. 1999; Benoist et al. 1999), while the central 5×5 arcmin area is also covered in *JK* from SOFI observations at the NTT. While we now also have *R*-band images these were not available at the time these observations were being prepared. For these clusters the targets were selected using one of the following criteria: *i)* using the photometric redshifts computed in the area covered by the infrared data (e.g., Arnouts et al. 1999); *ii)* searching for the expected $(I - K)$ and $(J - K)$ colours of early-type galaxies in the redshift interval of interest; *iii)* identifying *B*- and *V*-dropouts (expected for early-type galaxies considering the depth of EIS-WIDE) in the outer part of the field; and *iv)* arbitrarily to fill the slits (about 50% in the outer parts). When using the photometric redshifts, the targets were chosen within the redshift range $z \sim 0.6$–1.3. We used this broad interval due to the lack of *R*-band data which causes a large uncertainty (degeneracy) in the location of the 4000 Å break for galaxies in the interval $z \sim 0.5$–0.9. Furthermore, the errors in redshift estimates are $\sim$0.15 close to the magnitude limit of the sample. In the case of EIS0533-2412 only *IJK* data were available. In this case, the targets were selected by searching for the expected $(I - K)$ and $(J - K)$ colours of early-type galaxies in the redshift interval of interest. In the case of EIS0046-2930, expected to be at lower redshifts, galaxies were selected in the magnitude range of $19 \lesssim I_{AB} \lesssim 22.5$, while for EIS0533-2412 and EIS0954-2023 they were drawn in the interval $21 \lesssim I_{AB} \lesssim 23$.

A full description of the colour selection used to build the list of spectroscopic targets likely to be cluster members will be presented in a forthcoming paper (Jørgensen et al. in prep.).

3. VLT spectroscopy

The spectroscopic observations presented here were carried out using FORS1 in the MOS mode (September 2000) on the VLT-ANTU telescope and FORS2 in the MXU mode on the VLT-Kueyen telescope (December 2000) (cf. `http://www.eso.org/instruments`). In the MOS mode FORS1 provides 19 movable slit blade pairs that can be placed in the available field-of-view. For the present observations Grism 150I+17 with the order separation filter OG590 was used, providing a useful field of 4.7×6.8 square arcmin and covering the spectral range 6000–11000 Å. The dispersion of 230 Å/mm (5.52 Å/pixel) yielded a spectral resolution of 280 or about 29 Å for a slit width of 1.4 arcsec. The FORS2 observations were carried out in the multi-object (MXU) spectroscopy mode using GRISM 200I+28 with order separation filter OG550 covering the spectral range 5600–11000 Å. The dispersion of 162 Å/mm (3.89 Å/pixel) yielded a resolution of 380 or about 21 Å for a slit width of 1.2 arcsec. The slit mask allowed for a much larger multiplex than was possible with FORS1 and typically over 35 objects could be observed simultaneously.

The spectroscopic data were reduced using standard IRAF routines. The extracted one-dimensional spectra were then inspected to identify spectral features and obtain a preliminary redshift estimate. The spectra were then cross-correlated to template spectra using the FXCOR task of IRAF. In general, the differences between the three redshift estimates (emission lines, absorption features, and cross correlation) were small and the redshift measured by the cross-correlation was adopted. A more detailed account of the reduction procedure will be presented elsewhere (Jørgensen et al. in prep.).

A summary of the spectroscopic observations and the results obtained from the data analysis is presented in Table 1. Individual exposure times ranged from 900 to 1800 s depending on the total integration time required for each mask. Note that in the case of EIS0533-2412 two masks were prepared but

Table 1. Summary of the observations.

Candidate	date	seeing (arcsec)	Inst.	Nr. of masks	Integration time	Observed objects	Measured redshifts	Stars	No Identification
EIS0046-2930	24/09/2000	0.6–0.7	FORS1	4	3600 s	85	63	5	17
EIS0533-2412	25/12/2000	0.7–1.2	FORS2	1	14 400 s	47	30	4	13
EIS0954-2023	26/12/2000	0.5–0.7	FORS2	2	14 400 s	80	54	11	15

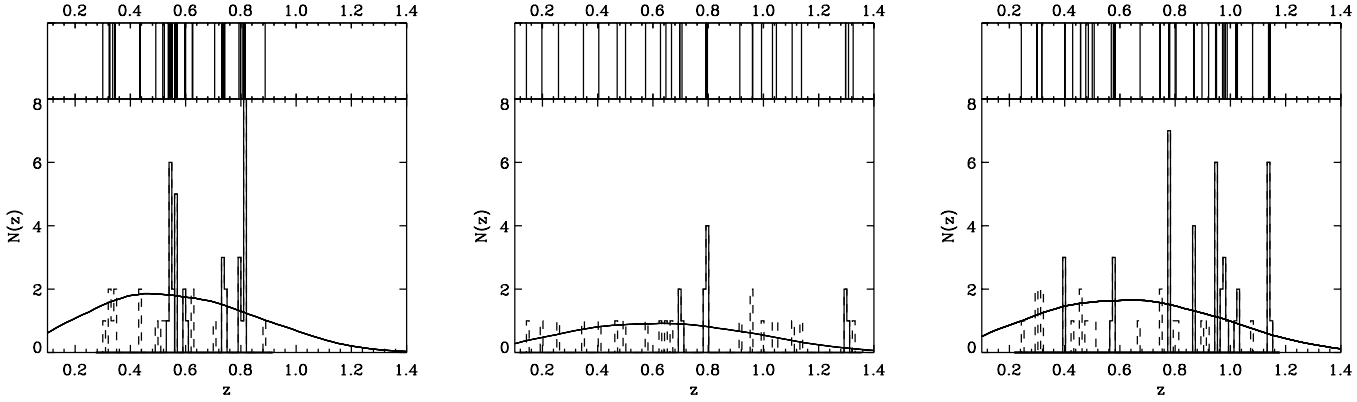

Fig. 1. Redshift distribution of galaxies in the fields of EIS0046-2930 (left), EIS0533-2412 (middle) and EIS0954-2023 (right). The upper part of the panels shows each individual measurement while in the lower part the measurements are grouped in bins $\Delta z = 0.01$ wide. The solid histograms indicate galaxy groups identified in redshift space as described in the text.

technical problems prevented the use of one of them at the time of the observation. In the case of EIS0954-2023 one of the masks was 30 min shorter. Altogether, a total of 212 objects were observed yielding 147 measured redshifts in the redshift interval 0.14–1.32.

4. Results

In Fig. 1 we present the distribution of measured redshifts for each of the fields considered showing in the upper part of each panel the individual redshifts and in the lower part the redshift distribution in bins $\Delta z = 0.01$ wide. The solid histograms indicate groups that have been identified from the analysis of the redshift distribution as discussed below. For each field the measured redshift distribution is compared to that expected for a uniform distribution of galaxies with a given luminosity function (LF) and selected in the same magnitude intervals as the observed galaxies. The *I*-band LF was computed using the LF parameters, split into three spectral classes (early, spiral and late-types), as derived from the *R*-band data of the ESO-Sculptor Survey (de Lapparent et al. in prep.) up to $z \sim 0.6$. We assumed that the LF remains constant at higher redshifts. The *I*-band LF at different redshifts was then obtained using the appropriate SEDs for the three spectral classes considered (Arnouts et al. in prep.). It was confirmed that this approach leads to a redshift distribution which is consistent with that measured by the CFRS survey when the same limiting magnitude is adopted. The predicted distribution is normalised by requiring the number of objects with $z > 0.5$ to be equal to the number of galaxies observed. This is done to approximately simulate the colour/photometric redshift criteria adopted in selecting the target galaxies.

From the figure one can immediately see the presence of several peaks in the observed distribution relative to the uniform background. Note that the redshift range covered by the observations of the EIS0046-2930 ($0.2 < z < 0.9$) is smaller than that for the other two cases which have measured redshifts up to $z \sim 1.3$. This is due to the brighter magnitude interval adopted in selecting the galaxy sample. This also explains the difference in the predicted redshift distribution for this field. It is also interesting to point out that while most of the redshifts lie beyond $z \sim 0.5$, as originally intended, some have lower redshifts. The fraction of galaxies with $z \lesssim 0.5$ is $\lesssim$10% of the total number of galaxies with redshifts, nearly all corresponding to faint ($I_{AB} \sim 21$–23) objects arbitrarily selected to fill-in available slits. Typically about 50% of the observed galaxy sample was arbitrarily selected, reflecting the fact that the area covered with infrared data (limited by the size of the SOFI field) was too small to position all the slits of the spectrograph.

Given the incompleteness of the sample, groups have been identified first in redshift space and then by their angular proximity. Groups in redshift-space have been identified using the "gap"-technique of Katgert et al. (1996) which identifies gaps in the redshift distribution larger than a certain size to separate individual groups. In this preliminary analysis we have adopted a redshift gap of $\Delta z = 0.005 * (1 + z)$ corresponding to 1500 km s^{-1} in the rest-frame. A total of five, three and eight groups with more than 3 members were found in the fields of EIS0046-2930, EIS0533-2412 and EIS0954-2023, respectively. To assess the significance of these detections we have resorted to simulations and evaluated how frequently peaks similar to those identified can occur by chance drawing galaxies with $z > 0.5$ from a uniform background. We find

Table 2. Groups identified in the cluster fields.

Candidate	RA	Dec	N_g	$\langle z \rangle$	σ (km s^{-1})
EIS0046-2930	00:46:29.6	−29:30:57.4	12	0.808	1171
EIS0533-2412	05:33:40.3	−24:12:43.8	3	1.301	-
EIS0954-2023a	09:54:47.5	−20:23:55.2	6	0.948	202
EIS0954-2023b	09:54:37.0	−20:22:54.7	8	1.141	285

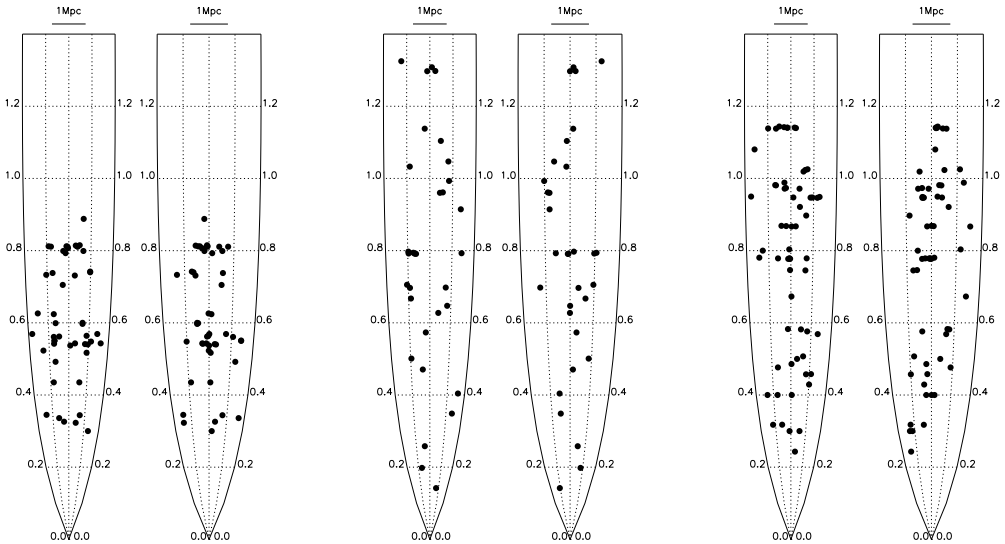

Fig. 2. Redshift versus right ascension (left) and declination (right) for the fields of EIS0046-2930, EIS0533-2412 and EIS0954-2023 corresponding to an angular scale of 10×10 arcmin. The scale of 1 Mpc corresponds to $z = 1.2$. The shape of the cones translates the evolution of that scale with redshift.

that 8 groups (2 in EIS0046-2930, 2 in EIS0533-2412 and 4 in EIS0954-2023), corresponding to 50% of the groups identified, are likely to correspond to real enhancements in redshift space (99% confidence level). In addition, we can also ask how many of these are also spatially concentrated. This can be done by examining Fig. 2 which shows, for each field, diagrams plotting redshifts as a function of right ascension and declination. From the figure it is easy to identify the most compelling cases of galaxies not only with concordant redshifts but also within a circular region roughly 1 arcmin in radius. These cases are listed in Table 2 which gives: in Col. 1 the name of the cluster; in Cols. 2 and 3 the Right Ascension and the Declination; in Col. 4 number of members; in Cols. 5 and 6 the mean redshift and the standard deviation in km s^{-1}. We remind the reader that all these cases are firm (99%) detections in redshift space and their location is in excellent agreement (<1 arcmin) with the position of the original candidate as identified by the matched-filter analysis.

In summary, in all three candidate cluster fields considered we identify at least one significant concentration of galaxies in redshift and in position. In the field of EIS0046-2930 we identify a system at $z = 0.808$. This candidate was originally assigned a matched-filter redshift of $z \sim 0.6$ but subsequent work using optical/infrared colour-magnitude diagrams (da Costa et al. 1999) suggested it to be at higher redshift. Indeed, the apparently brightest galaxy in the cluster was measured to be at $z = 0.81$ (Ramella, private communication). New measurements of another 11 galaxies with concordant redshifts now corroborate this earlier result. In the field of EIS0533-2412 we find a significant concentration at $z = 1.3$, which coincides with the location of the matched-filter detection at an estimated redshift of $z = 1.1$. While currently only three galaxies have measured redshifts in the $z = 1.3$ system, most of the faint galaxies in the field have similar colours as shown in Fig. 3. Furthermore, recent analysis of an XMM-Newton image finds a $> 5\sigma$ detection centred near the location of the brightest cluster member for which we have a secure redshift at $z = 1.3$. In fact, the distribution of galaxies with similar $(J - K)$ colour extends some 3 arcmin to the NE, where another X-ray detection has been found. A more detailed discussion of the X-ray data will be presented elsewhere (Neumann et al. in prep.). Finally, in the field of EIS0954-2023 we find evidence for two clumps. One at $z = 1.141$, at the same location as the matched-filter detection, and the other a foreground concentration at $z = 0.95$, some 2 arcmin away from the original detection. High resolution cutouts for the systems discussed here can be found at the URL "`http::www.obs-nice.fr/benoist/high-z.clusters.html`".

5. Summary

This paper presents new spectroscopic data of EIS cluster candidate fields identified from moderately deep I-band images using the matched-filter algorithm. The three fields considered were selected because the cluster candidates had estimated redshifts beyond $z = 0.8$. Analysis of the spectroscopic data

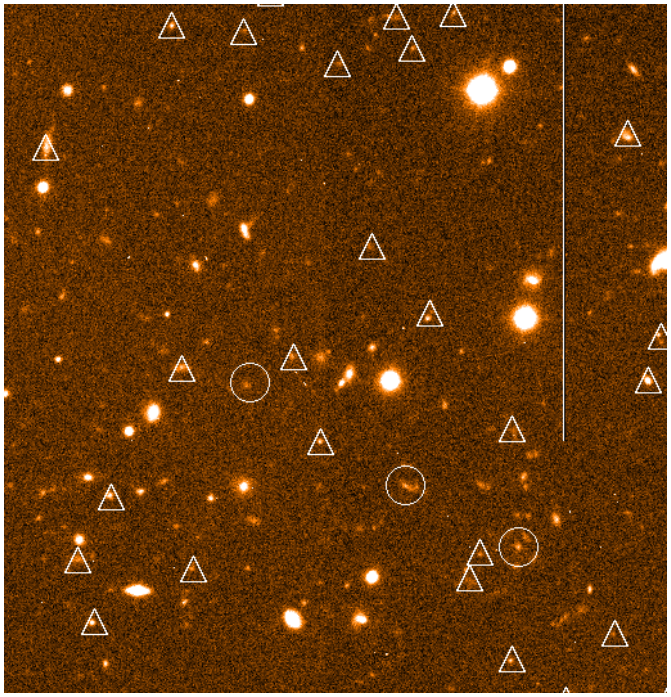

Fig. 3. Image cutout 2 arcmin to the side taken from a FORS *R* image of the cluster field EIS0533-2412. Circles show galaxies with similar spectroscopically confirmed redshift, while triangles those with similar colours. Note the concentration of faint galaxies near the lower right corner.

strongly suggests the existence of real density enhancements at high redshifts ($0.8 < z < 1.3$) in all of them. The measured redshifts are, in general, consistent with those estimated from the photometric data. In at least one of the cluster fields, the location of the high-redshift system coincides remarkably well with a robust X-ray detection, lending further support to the reality of the system. Therefore, despite the fact that it is difficult to decide if those clumps are filaments or bound systems, for two of them the evidence seem to favour the second possibility: for the $z = 0.81$ clump a red sequence is observed (da Costa et al. 1999) whereas the $z = 1.3$ one has an X-ray detection associated with it.

The present paper strongly suggests that the EIS cluster candidate catalog provides a valuable pool from which to construct a statistical sample of optically-selected clusters at high redshift. The present data alone contribute with four systems at $z > 0.8$ in the southern hemisphere, two of which at $z \gtrsim 1$, ideal for VLT studies. The success in identifying significant concentrations from a relative small sample underscores the importance of collecting multi-band optical/infrared data and estimating photometric redshifts to select potential cluster members. However, in establishing the true nature of these systems will require a better sampling of these systems which will become possible with the availability of an integral field unit as foreseen by the VIMOS spectrograph.

Acknowledgements. We would like to thank the EIS Team for the effort of producing the publicly available object catalogs for the EIS-Wide and Pilot Surveys. LFO thanks the SARC and Carlsberg Foundations for financial support during the project period.

References

Arnouts, S., Cristiani, S., Moscardini, L., et al. 1999, MNRAS, 310, 540
Benoist, C., da Costa, L., Olsen, L. F., et al. 1999, A&A, 346, 58
Carlstrom, J. E., Joy, M. K., Grego, L., et al. 2000, Phys. Scr., 85, 148
da Costa, L. N., Scodeggio, M., Olsen, L., et al. 1999, A&A, 343, 29
Gioia, I. 2000, Constructing the Universe with Clusters of Galaxies, IAP 2000 meeting, ed. F. Durret, & D. Gerbal
Gladders, M. D., & Yee, H. K. C. 2000, AJ, 120, 2148
Gonzalez, A. H., Zaritsky, D., Dalcanton, J., et al. 2001, ApJS, 137, 117
Gunn, J. E., Hoessel, J. G., & Oke, J. B. 1986, ApJ, 306, 30
Katgert, P., Mazure, A., Perea, J., et al. 1996, A&A, 310, 8
Nonino, M., Bertin, E., da Costa, L., et al. 1999, A&AS, 137, 51
Olsen, L., Scodeggio, M., da Costa, L., et al. 1999a, A&A, 345, 363
Olsen, L., da Costa, L. N., Scodeggio, M., et al. 1999b, A&A, 345, 681
Olsen, L. F., Benoist, C., da Costa, L. N., et al. 2001, A&A, 380, 460
Postman, M., Lubin, L. M., Gunn, J. E., et al. 1996, AJ, 111, 615
Ramella, M., Biviano, A., Boschin, W., et al. 2000, A&A, 360, 861
Rosati, P., Stanford, S. A., Eisenhardt, P. R., et al. 1999, AJ, 118, 76
Scodeggio, M., Olsen, L. F., da Costa, L., et al. 1999, A&AS, 137, 83
Stanford, S. A., Elston, R., Eisenhardt, P. R., et al. 1997, AJ, 114, 2232